Diagnostics for Plasma Enhanced Chemical Vapor Deposition and Etch Systems

Final Report
NASA Ames University Consortium Grant NCC2-5205

Grant end date: January 31, 1999

Prepared by:

Prof. Mark A. Cappelli
Mechanical Engineering Department
Stanford University
Stanford, CA 904305-3032

Prepared for:

NASA Ames University Consortium
Mail Stop 241-1
NASA-Ames Research Center
Moffett Field, CA 94035-1000

July 2, 1999

1. Executive Summary

In order to meet NASA's requirements for the rapid development and validation of future generation electronic devices as well as associated materials and processes, enabling technologies ion the processing of semiconductor materials arising from understanding etch chemistries are being developed through a research collaboration between Stanford University and NASA-Ames Research Center.

Although a great deal of laboratory-scale research has been performed on many of materials processing plasmas, little is known about the gas-phase and surface chemical reactions that are critical in many etch and deposition processes, and how these reactions are influenced by the variation in operating conditions. In addition, many plasma-based processes suffer from stability and reliability problems leading to a compromise in performance and a potentially increased cost for the semiconductor manufacturing industry. Such a lack of understanding has hindered the development of process models that can aid in the scaling and improvement of plasma etch and deposition systems.

The research described involves the study of plasmas used in semiconductor processes. An inductively coupled plasma (ICP) source in place of the standard upper electrode assembly of the Gaseous Electronics Conference (GEC) radio-frequency (RF) Reference Cell is used to investigate the discharge characteristics and chemistries. This ICP source generates plasmas with higher electron densities (~ 10^{12}/cm^3) and lower operating pressures (~ 7 mTorr) than obtainable with the original parallel-plate version of the GEC Cell. This expanded operating regime is more relevant to new generations of industrial plasma systems being used by the microelectronics industry.

The motivation for this study is to develop an understanding of the physical phenomena involved in plasma processing and to measure much needed fundamental parameters, such as gas-phase and surface reaction rates, species concentration, temperature, ion energy distribution, and electron number density. A wide variety of diagnostic techniques are under development through this consortium grant to measure these parameters, including molecular beam mass spectrometry (MBMS), Fourier transform infrared (FTIR) spectroscopy, broadband ultraviolet (UV) absorption spectroscopy, a compensated Langmuir probe. Additional diagnostics, such as microwave interferometry and microwave absorption for measurements of plasma density and radical concentrations are also planned.

In this report, details of the GEC discharge cell setup and each diagnostic technique fabricated during the grant period are described. A description of the GEC Cell facility is presented in Section 2. The facility includes a basic GEC Reference Cell vacuum chamber, mechanical and turbomolecular pumps, matching networks, and RF power supplies. Section 3 presents the setup for mass spectrometry. Detailed descriptions for FTIR and UV absorption measurements are presented in Sections 4 and 5. The design of a compensating Langmuir probe and data analysis method are discussed in Section 6.

2. GEC RF Reference Cell

A schematic of the GEC Cell facility is shown in Figure 1. The entire GEC Cell, including main chamber, manifold, and ports, are constructed of stainless-steel ultrahigh vacuum components. Eight ports (two 8" ports, two 6" ports, and four 2.75" ports) are arranged around the mid-plane of the GEC Cell to provide easy access for diagnostic measurements and instrument installations.

Source gases are supplied through the 6" port, and pumped out by a rotary vane pump (Leybold D40BCS, 40 m^3/h) which is connected to the symmetric pumping manifold at the bottom of the GEC Cell. A roots vacuum pump (Leybold WS 251) is also used to shift the operating pressure into the high vacuum range and to increase the pumping speed. A turbomolecular pump (Pfeiffer TPU 270, 270 liter/s), backed up by a mechanical pump (Leybold D16B, 16.5 m^3/h) is installed directly to one of the 6" ports and base pressures near 1.5×10^{-8} Torr are achieved.

The inductive coil is a five-turn, approximately 3.5" in diameter, planar coil constructed from 1/8" diameter copper tubing. The coil is separated from the plasma by a quartz window (0.375" in thickness and 5" in diameter). The coil is powered by a 13.56 MHz RF power supply (Advanced Energy RFXII 1250) and a matching network (Lam Research Corporation) consisting of two air-dielectric variable capacitors, is mounted directly to the coil to minimize resistive losses. A plane, 10 cm in diameter, stainless steel lower-electrode is biased by a 13.56 MHz RF power supply (Comdel CPS 1001S) and an impedance matching network (Comdel CPMX-2500). Both matching networks are tuned for minimum reflected power for each plasma condition by either manual or automatic control. The reflected power is always in the range of 0 – 4 W. A high voltage probe (TEKTRONIX P6015A) monitors the coil voltage and a Hall probe (Pearson 5673) monitors the coil current. The lower electrode voltage and root-mean square discharge current is also monitored with a voltage probe (Tektronix P5100) and a Hall probe (Pearson 2878). Voltage and current are recorded using two-channel digital oscilloscopes (Tektronix TDS 340A and 2440). The distance between the quartz window and lower electrode is approximately 1.4".

The gas flow rates are kept constant by using mass flow controllers (Tylan General FC-2900M for Ar and DFC-2900M for CHF_3 and CF_4). The pressure is monitored with an ion gauge and a Baratron absolute pressure gauge (MKS 122 B). An exhaust throttle valve (MKS 253 B) which is installed between the GEC Cell and the mechanical pump controls the gas flow out of the GEC Cell. The pressure in the GEC Cell is controlled by a personal computer using the LabVIEW programming software.

3. Mass Spectrometry

A mass spectrometer is an apparatus, which produces a beam of gaseous ions from a sample, sorts out the resulting mixture of ions according to their mass-to-charge ratios, and provides output signals, which are measures of the relative abundance of each ionic species present in the chamber sampled. System interpretation of the mass and energy spectra provides a detailed picture of the complex ionization and chemical processes in plasmas, and the interaction of the plasmas with surfaces/electrodes. In reactive plasmas, ion bombardment of a surface during the processing of semiconductor materials plays a major role in depositing materials and also etching the fine features in device integration. Consequently, determination of the energies and identity of each ionic species is critical to develop new tools that can provide layer-by-layer control of the removal and addition of materials of nanometer dimensions.

The mass spectrometer is embedded in the lower (independently biased) electrode as shown in Figure 1. The Hiden EQP (Electrostatic Quadrupole Plasma) analyzer employed in this study

is a high-transmission 45° sector field ion energy analyzer and quadrupole mass spectrometer designed as a diagnostic tool for plasma or SIMS analysis. Mass spectra, energy spectra, and appearance potential profiles can be acquired, allowing detailed analysis of positive ions, negative ions, radicals, and neutrals.

The EQP probe comprises the following items:

- An ion extraction system.
- A twin-filament, fully-adjustable electron-impact ion source for RGA (Residual Gas Analyzer) of neutrals and radicals. The ion extractor and ion source are protected by a cover tube which has a small sampling orifice connecting to the plasma chamber for ion and gas inlet. The probe is pumped to operating pressures by its own turbomolecular pump. The ion source is located as close as possible to the sampling orifice for efficient analysis of neutrals and radicals.
- A 45° electrostatic field energy filter for energy analysis.
- A triple-section quadrupole mass filter for mass-to-charge ratio analysis.
- A detector. The detector is an ion counting SEM (Secondary Electron Multiplier) which counts the number of ions striking it per second. It gives high sensitivity with a low background count rate, and in operation, a high voltage of 1.5 to 3.0 kV is applied across the detector.

A lower electrode with a 30 μm orifice is integrated electrically and mechanically with the EQP system. It is surrounded by a grounded shield and can be either rf-powered or grounded. The lower electrode is water-cooled to prevent the pressure rise in the EQP system, which is limited to approximately 5×10^{-6} Torr.

The mass spectrometer is fully functional, and preliminary studies have been performed on pure argon plasmas. The total ion flux densities measured in argon plasmas for a range of pressures and incident power levels are shown in Figure 2. The results indicate that ion flux increases with operating pressure and incident power, in good agreement with previous studies performed at other laboratories. Figure 3 shows the measured ion flux distributions (IFDs) for Ar^+ ions in argon plasmas for pressures ranging from 10 mTorr to 50 mTorr for 100 W and 300 W. The magnitude of each IFD has been scaled to the total ion current densities shown in Figure 2. The IFDs exhibit the relatively narrow shape, well separated from zero energy, which is in contrast to IFDs measured in capacitively coupled plasmas. The IFDs in capacitively coupled plasmas show a continuum of ion energies extending down to near zero energy. Figure 4 shows the variation in the mean ion energy as a function of operating pressure for three different incident powers. The mean ion energies exhibit very strong pressure dependence, however, the mean ion energies are nearly independent of incident power.

4. Fourier Transform Infrared Spectroscopy

In situ, real-time, infrared diagnostic studies of the evolution of gas-phase species in the chemical vapor deposition (CVD) reactor has become a critical component in the development and optimization of manufacturable CVD processes, both scientifically and industrially. Scientifically, such studies are required to establish the underlying mechanisms of reactant gas-phase evolution and their effects on precursor decomposition and film formation. Industrially, emerging manufacturable processes require accurate and nonintrusive tools for in situ monitoring of the gas-phase evolution of reactants in the CVD reactor and providing critical adjustments for optimal film quality.

In low pressure discharges using source gases such as CF_4 and CHF_3, the detection of CF_x (x = 1-3) radicals is of importance to the understanding of their chemical structure and relevance in reactive ion etching. These radicals are known to contribute to the formation of fluorocarbon

polymer films, which affect the selectivity and anisotropy of etching. In this study, Fourier transform infrared (FTIR) spectroscopy is employed to observe the absorption band of CF_3 radicals in the electronic ground state X^2A_1 in the region of 1233 – 1270 cm^{-1}.

A schematic of the experimental setup is shown in Figure 5. A Nicolet Magna-IR 560 FTIR optical bench is employed for nonintrusive infrared absorption measurements. This FTIR system provides continuous dynamic alignment for exceptional long-term spectral stability, interactive parameter selection with instantaneous feedback of changes to scanning velocity, signal gain, and optical output, and real-time system diagnostics. The Magna-IR 560, which has a fixed resolution of 0.125 cm^{-1}, consists of an IR light source, a potassium bromide (KBr) beam splitter, a reflective mirror, a Michelson interferometer, and a liquid nitrogen cooled, high sensitivity HgCdTe (MCT) detector. A helium-neon laser is employed as an internal reference and for calibration. The high-intensity, Ever-Glo mid-infrared source requires no external utilities, and is stable and extremely reliable. An automated, continuously variable aperture optimizes energy from the infrared source.

The IR beam is transmitted through the GEC Cell (two diametrically opposite potassium bromide windows mounted on 2.75" Conflat flanges) and collected by the IR detector through a line-of-sight configuration. The optical bench is purged with dry air to prevent undesirable artifacts from atmospheric carbon dioxide and water vapor which may lead to significant reduction in IR beam intensity and serious interference in the absorption spectra. A dry air purged plastic box is used as the conduit for IR light between the optical bench and the GEC Cell. The facility is now fully operational, and we expect to begin testing the in-situ FTIR capabilities within the next funding period.

5. UV Absorption Spectroscopy

Many radicals of interest in etch chemistries have strong ultraviolet absorption signatures which can be identified by ultraviolet absorption spectroscopy. The quantitative measurement of radical concentrations and their spatial distributions provide a test of theoretical models that describe the kinetics of plasma discharges and their ability to predict the overall reactor-scale performance. During this grant period, we have carried out preliminary feasibility studies related to the quantitative detection of methyl radicals (CH_3) and difluorocarbene radicals (CF_2), which are products of electron collisional dissociation of methane (CH_4) and tetrafluoromethane (CF_4) in low-pressure RF plasma discharges. The CH_3 detection method employed in these experiments relies on the relatively well studied, ultra-violet absorption bands of methyl near 216 nm, corresponding to the $X(^2A_2'') \rightarrow B(^2A_1')$ electronic transition. This transition is generally featureless, as the upper state is pre-dissociated. The absolute absorption coefficient and its temperature dependence have been previously measured [1, 2]. The CF_2 detection method employed uses the less studied, ultra-violet absorption bands near 240 nm, corresponding to the $X \rightarrow A$ electronic transition [3]. The ro-vibronic structure for this transition is not resolved in this study. The absolute absorption coefficient has been previously estimated at a wavelength of 249.8 nm [4].

The use of broadband ultraviolet absorption measurements as a relatively simple, novel method for quantitative studies of methyl radical concentration in low pressure discharges and thermal CVD environments was first reported by Childs, *et al* [5]. In the application of this diagnostic, a bright source of broadband ultraviolet emission of intensity $I_{o\lambda}$, centered about the wavelength of interest, λ, is directed through a plasma containing CH_3 radicals (or CF_2) of concentration n_{CH3} (or n_{CF2}) that is assumed uniform along the line-of-sight. The Beer-Lambert

law is used to extract the column density, $n_{CH3}L$, which is the product of methyl number density and discharge path length along which the intense ultraviolet beam traverses:

$$n_{CH3}L = \frac{\chi_{CH3}PL}{k_B T} = -\frac{1}{k_\lambda k_B T}\ln\frac{I_\lambda}{I_{o\lambda}} \qquad (1)$$

Here, k_B is the Boltzmann constant, T is the temperature, I_λ is the transmitted ultraviolet bean intensity, and k_λ is the temperature-dependent spectral absorption coefficient for the transition. In Eqn.1, the methyl density is also expressed in terms of the methyl mole fraction, χ_{CH3}, where the total discharge pressure is P. The spectral absorption coefficient for the $X(^2A_2'') \rightarrow B(^2A_1')$ electronic transition and its temperature dependence at peak absorption, 216.4 nm, has been measured by Davidson, *et al* [1,2], and is given here as:

$$k_\lambda = 1.47\times10^5 T^{-1}\exp(-T/1675) \qquad (\text{atm}^{-1}\text{cm}^{-1}) \qquad (2)$$

where T is the temperature in Kelvin. More recently, Kumaran, *et al* [4], have estimated the spectral absorption cross section, σ_λ, at 249.8 nm for the $X \rightarrow A$ electronic transition in CF_2 to be:

$$\sigma_\lambda = 2.26\times10^{-18} \qquad (\text{cm}^2) \qquad (3)$$

This cross section corresponds to an absorption coefficient of:

$$k_\lambda = 1.64\times10^{-4}T^{-1} \qquad (\text{atm}^{-1}\text{cm}^{-1}) \qquad (4)$$

where again, T is the temperature in Kelvin. The temperature dependence of the absorption coefficient given here for CF_2 arises directly from the conversion, as no temperature dependence for the cross section is given in Ref. 4.

A schematic of the UV absorption experimental facility, as seen from above is shown in Figure 6. Broadband ultraviolet emission from an ultra-stable deuterium lamp (Oriel, Model 63162) is imaged, with a magnification of 0.3 using a 100mm focal length lens, onto a plane intersecting the center of the plume. The lamp emission is then re-imaged with a magnification of 2 (again using a 100 mm focal length lens) onto the entrance of a UV-grade silica optical fiber. The fiber caries the radiation to the 10 μm-wide entrance slit of compact linear CCD-array equipped spectrometer (Ocean Optics Model PC1000) having a 0.3 nm spectral resolution and sensitive to the 200-380 nm region of the UV-visible spectrum.

Scans are acquired using an interface software driver developed by the manufacturer. The spectrometer is capable of performing on-board dynamic averaging to a maximum 30 scans. An unlimited number of static averaging of spectral scans can be achieved by user-driven software

commands. On-chip spectral integration (per scan) can be set over the range of approximately 10-4000 msec.

A typical series of transmission spectra taken in a pure CH_4 ICP discharge over a wavelength range between 210 and 221 nm is shown in Figure 7. In this example, the coil power was varied between 75 and 500 W, the lower electrode power was 40W, the CH_4 flow rate was 23 sccm, and the chamber pressure was 40 mTorr. In this example, the spectra are internally processed by the spectrometer driving software to subtract dark noise (from a spectrum taken with the fiber blocked), and to divide each spectral scan by the background reference spectrum (taken with the discharge off). The total duration of the acquired data was approximately 3 minutes. We see that there is a clear evidence of methyl absorption centered at approximately 216 nm, the strength of which varies with coil power. The methyl concentration (path averaged) is estimated using an assumed optical path length of 10 cm, the size of the visible plasma. The inferred variation in the path-averaged methyl concentration with power is shown in Figure 8.

Typical transmission spectra taken in a CF_4/Ar discharge over a wavelength range between 230 and 290 nm is shown in Figure 9. For this example, the lower electrode power was at 90W and the coil power was either off, or set at 150W. Features attributed to CF_2 absorption are identified. Assuming a temperature of 300K and an optical path length of 10 cm, an estimated CF_2 path-averaged number density of 5×10^{12} cm^{-3} is obtained with the coil powered. A refinement of the UV absorption diagnostic for fluorocarbon discharges will continue in the next grant period.

6. Compensated Langmuir Probe Diagnostics

Knowledge of key plasma parameters, such as electron/ion number density, electron temperature, and electron energy distribution (EEDF) is required to develop an understanding of the physics and chemistry of plasma etching. Langmuir probes are widely used for the plasma characterization, since no other single measurement technique can provide quantitative information on species number densities, temperatures, plasma potential, and electron energy distributions simultaneously. In addition, it is relatively inexpensive and straightforward to implement. In RF plasmas, however, compensation of the probe is needed to account for the time-varying plasma potential. The compensation is achieved by designing a parallel resonance circuit into the probe. With such a circuit, the impedance to the rf signal is large, and the probe tip is therefore driven at the local plasma potential. An applied dc potential is thus superimposed on the floating rf potential, and the variation in this dc potential maps out the V-I characteristics of the probe. Note, however, that this V-I characteristic reflects the time-average plasma properties in the vicinity of the probe tip. A recent study of the use of such compensated probes in an ICP source built onto a GEC reference cell shows that the electron density derived from these probes for a pure argon plasma compare favorably with measurements made using microwave interferometry [6]. Measurements of plasma properties using compensated probes have also been made in rf discharges of other noble and non-reacting gases [7]. Only recently, however, have attempts been made to measure plasma properties in reacting gases such as CH_4, CF_4, and CHF_3. In such gases, contamination of the probe tip, and the lack of a suitable ground reference (as the reactor walls become coated) makes the interpretation of such measurements tenuous.

During this first phase of the research, we have designed and fabricated a compensated Langmuir probe, and have performed a preliminary characterization of pure argon ICP plasmas (with a grounded lower electrode). Examples of the plasma properties derived from this probe are shown in Figures 10-12. These measurements are in relatively good agreement with those

obtained previously [6]. An extensive data set on pure argon plasmas as well as molecular plasmas will be collected during the next phase of this program.

Summary

During this grant period, we have instrumented the GEC discharge cell with a variety of optical and probe diagnostics, including FTIR and UV absorption, Mass Spectrometry, and Langmuir probes. Preliminary measurements have been made in both non-reactive and reactive gas discharges, and results have been reported at international conferences. During the next grant period, a refinement of all of these measurement methods will be made, and extensive characterization of plasma chemistries of interest to the etch plasma community will be carried out. In addition, during the next grant period, the development of a new microwave diagnostic will be investigated.

Conferences Papers Presented

"Langmuir Probe Measurements in an Inductively Coupled GEC Reference Cell Plasma," J.S. Ji, J.S. Kim, M.A. Cappelli, and S.P. Sharma," 51st Annual Gaseous Electronics Conference, American Physical Society, Maui, HI, October 19-22, 1998. See also Bull. Am. Phys. Soc. **43**, 1424, 1998.

"Ion Energy Distributions and their Relative Abundance in Inductively Coupled Plasmas," J.S. Kim, M.V.V.S. Rao, M.A. Cappelli, and S.P. Sharma," 51st Annual Gaseous Electronics Conference, American Physical Society, Maui, HI, October 19-22, 1998. See also Bull. Am. Phys. Soc. **43**, 1426, 1998.

"CH3 and CFx Detection in Low Pressure RF Discharges by Broadband Ultraviolet Detection Spectroscopy," M.A. Cappelli, J.S. Kim, and S.P. Sharma," 51st Annual Gaseous Electronics Conference, American Physical Society, Maui, HI, October 19-22, 1998. See also Bull. Am. Phys. Soc. **43**, 1459, 1998.

References

1. D.F. Davidson, A.Y. Chang, M.D. DiRosa, and R.K. Hanson, JQSRT **49**, 559, (1993).
2. D.F. Davidson, M.D. DiRosa, E.J. Chang, and R.K. Hanson, JQSRT **53**, 581, (1995).
3. J.P. Booth, G. Hancock, N.D. Perry, and M.J. Toogood, J. Appl. Phys. **66**, 5251, (1989).
4. S.S. Kumaran, M.-C. Su, K.P. Lim, J.V. Michael, and A.F. Wagner, in preparation.
5. M.H. Childs, K.L. Menningen, P. Chevako, N.W. Spellmeyer, L.W. Anderson, and J.E. Lawler, Phys. Lett. A **171**, 87, (1992).
6. L. J. Overzet and M. B. Hopkins, J. Appl. Phys. **74** (7), 4323 (1993).
7. A. Schwabedissen, E. C. Benek, and J. R. Roberts, Phys. Rev. E **55**, 3450 (1997).

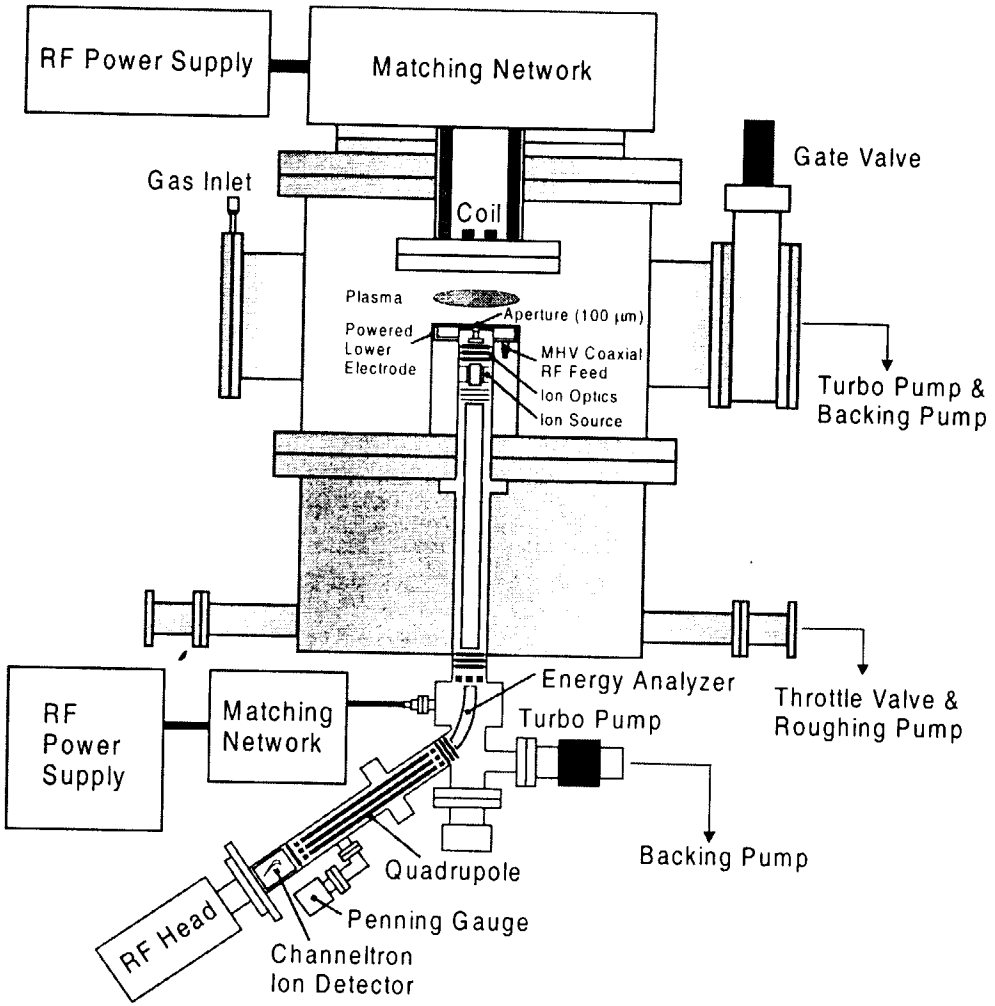

Figure 1. Schematic of the experimental facility, including the diagnostics capabilities that were developed during this grant period.

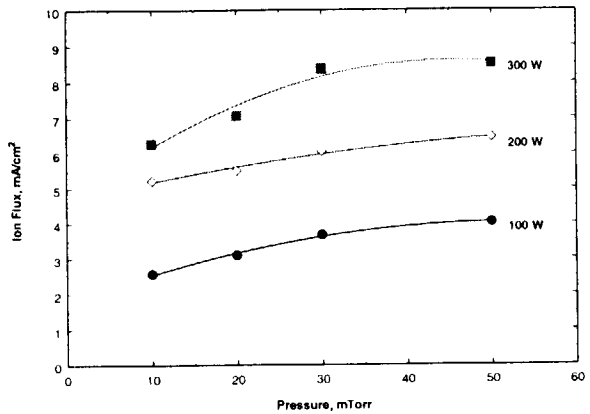

Figure 2. Ion flux variation with plasma chamber pressure. Lower electrode is grounded

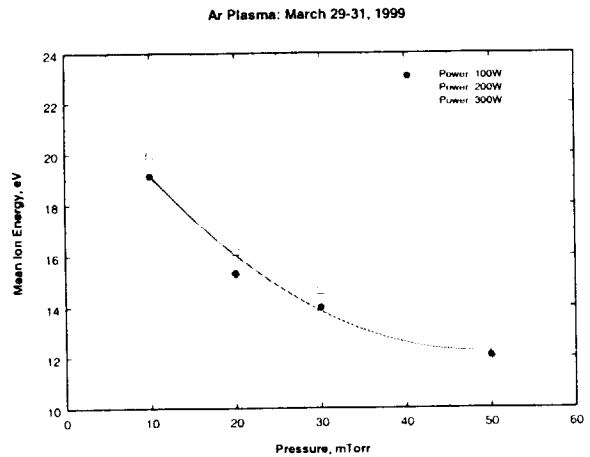

Figure 4. Mean ion energy verses discharge Pressure.

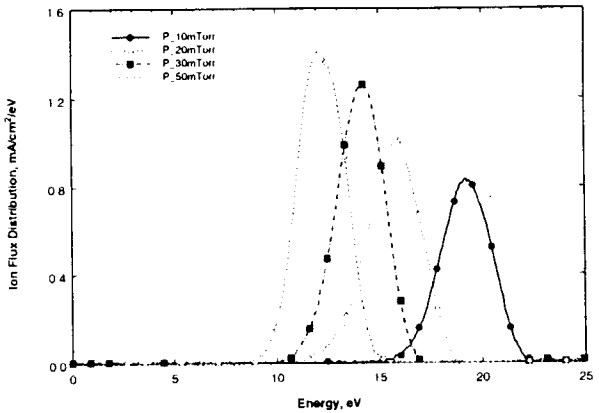

Figure 3 (a)

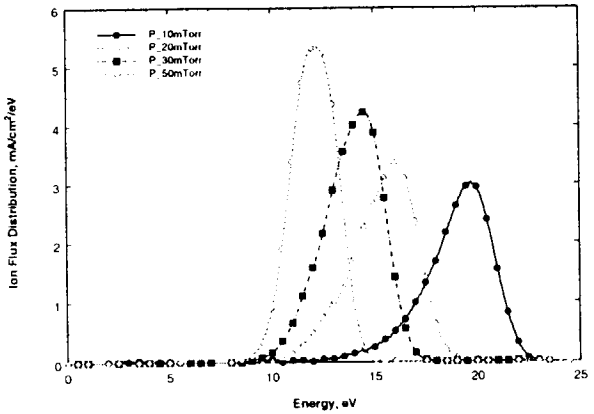

Figure 3 (b)

Figure 3. Ion flux variation with plasma chamber pressure. Lower electrode is grounded. (a): 100W (b) 300W discharge power.

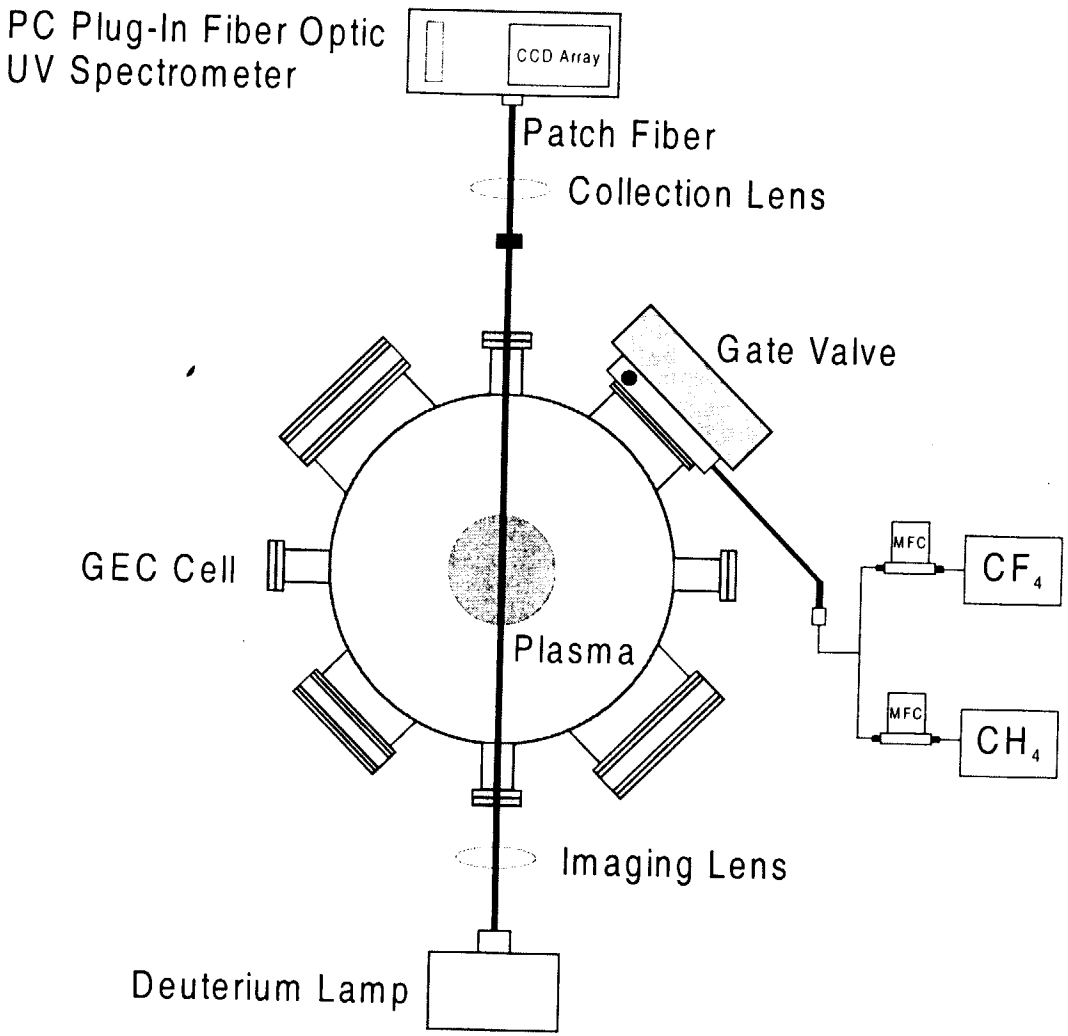

Figure 6. UV Absorption Setup

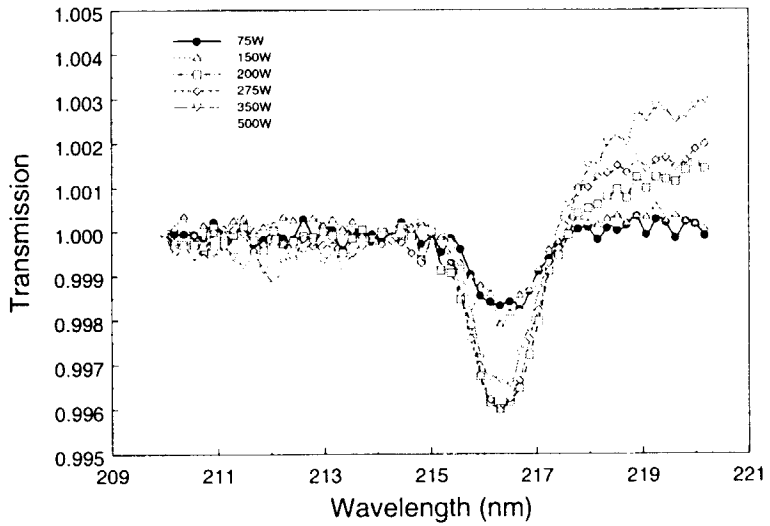

Figure 7. Methyl absorption spectra at various coil powers. Pressure = 40mTorr, methane flow rate = 23 sccm, lower electrode power = 40W

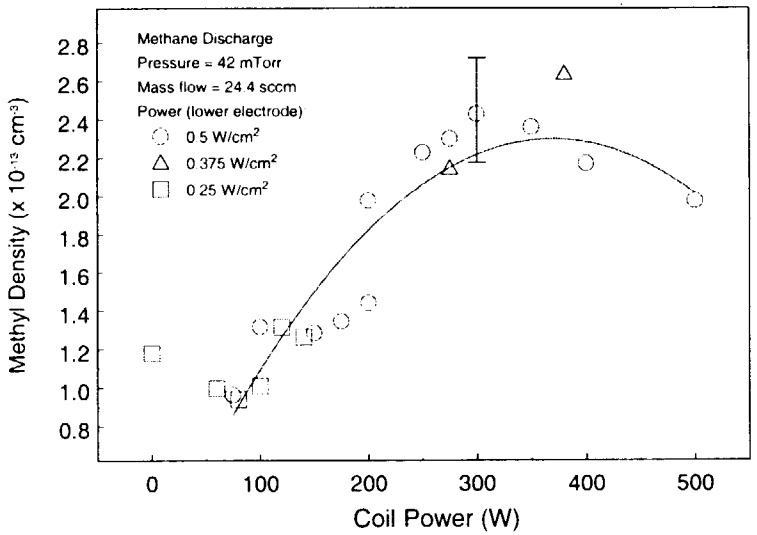

Figure 8. Methyl concentrations at various coil powers. Pressure = 40mTorr, methane flow rate = 23 sccm, lower electrode power = 40W

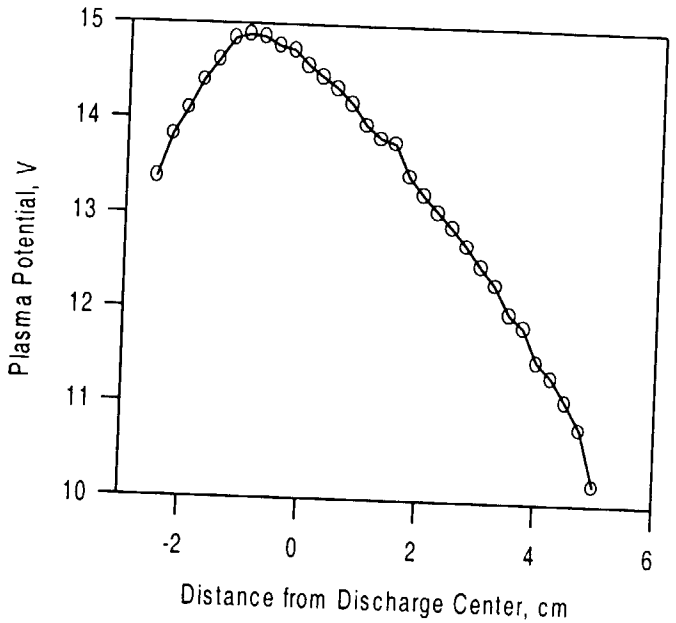

Figure 11. Radial variation in the plasma potential (same conditions as Fig. 10)

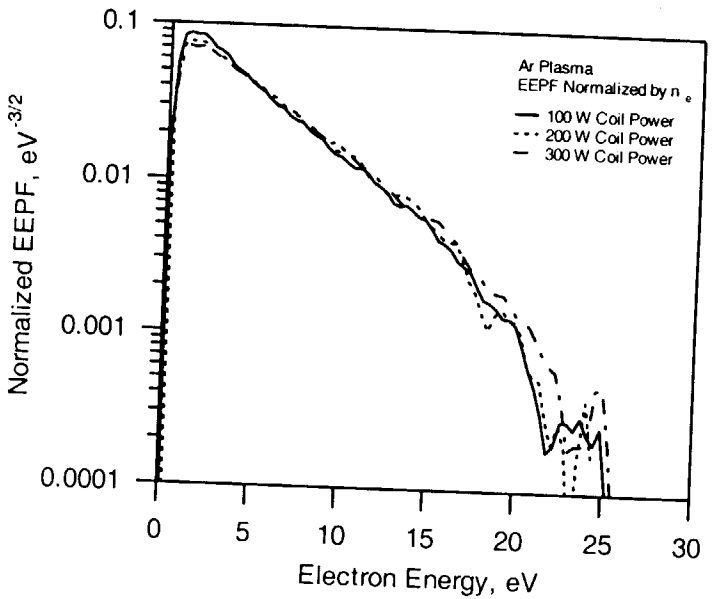

Figure 12. The EEPF at the center of the discharge (same conditions as Fig. 10, except p = 10mTorr)